

An all-optical phase detector by amplitude modulation of the local field in a Rydberg atom-based mixer

Xiu-Bin Liu(刘修彬), Feng-Dong Jia(贾凤东), Huai-Yu Zhang(张怀宇), Jiong Mei(梅炅),Wei-Chen Liang(梁玮宸), Fei Zhou(周飞), Yong-Hong Yu(俞永宏), Ya Liu(刘娅), Jian Zhang(张剑), Feng Xie(谢锋), and Zhi-Ping Zhong(钟志萍)

Citation: Chin. Phys. B, 2022, 31 (**9**): 090703. DOI: 10.1088/1674-1056/ac6dbb
Journal homepage: http://cpb.iphy.ac.cn; http://iopscience.iop.org/cpb

What follows is a list of articles you may be interested in

Optoelectronic oscillator-based interrogation system for Michelson interferometric sensors

Ling Liu(刘玲), Xiaoyan Wu(吴小龑), Guodong Liu(刘国栋), Tigang Ning(宁提纲), Jian Xu(许建), and Haidong You(油海东)

Chin. Phys. B, 2022, 31 (**9**): 090702. DOI: 10.1088/1674-1056/ac4f59

Numerical study of a highly sensitive surface plasmon resonance sensor based on circular-lattice holey fiber

Jian-Fei Liao(廖健飞), Dao-Ming Lu(卢道明), Li-Jun Chen(陈丽军), and Tian-Ye Huang(黄田野)

Chin. Phys. B, 2022, 31 (**6**): 060701. DOI: 10.1088/1674-1056/ac43a5

A stopping layer concept to improve the spatial resolution of gas-electron-multiplier neutron detector

Jianjin Zhou(周建晋), Jianrong Zhou(周健荣), Xiaojuan Zhou(周晓娟), Lin Zhu(朱林), Jianqing Yang(杨建清), Guian Yang(杨桂安), Yi Zhang(张毅), Baowei Ding(丁宝卫), Bitao Hu(胡碧涛), Zhijia Sun(孙志嘉), Limin Duan(段利敏), and Yuanbo Chen(陈元柏)

Chin. Phys. B, 2022, 31 (**5**): 050702. DOI: 10.1088/1674-1056/ac398e

Finite element simulation of Love wave sensor for the detection of volatile organic gases

Yan Wang(王艳), Su-Peng Liang(梁苏鹏), Shu-Lin Shang(商树林),Yong-Bing Xiao(肖勇兵), and Yu-Xin Yuan(袁宇鑫)

Chin. Phys. B, 2022, 31 (**3**): 030701. DOI: 10.1088/1674-1056/ac3ec9

Effect of staggered array structure on the flow field of micro gas chromatographic column

Daohan Ge(葛道晗), Zhou Hu(胡州), Liqiang Zhang(张立强), and Shining Zhu(祝世宁)

Chin. Phys. B, 2022, 31 (**1**): 010701. DOI: 10.1088/1674-1056/ac0902

An all-optical phase detector by amplitude modulation of the local field in a Rydberg atom-based mixer

Xiu-Bin Liu(刘修彬)[1], Feng-Dong Jia(贾凤东)[1], Huai-Yu Zhang(张怀宇)[1,2], Jiong Mei(梅炅)[1,2], Wei-Chen Liang(梁玮宸)[1], Fei Zhou(周飞)[1], Yong-Hong Yu(俞永宏)[1,2], Ya Liu(刘娅)[3], Jian Zhang(张剑)[4], Feng Xie(谢锋)[4,†], and Zhi-Ping Zhong(钟志萍)[1,5,‡]

[1] *School of Physical Sciences, University of Chinese Academy of Sciences, Beijing* 100049, *China*
[2] *Institute of Physics, Chinese Academy of Sciences, Beijing* 100190, *China*
[3] *National Time Service Centre, Chinese Academy of Sciences, Xi'an* 710600, *China, University of Chinese Academy of Sciences, Beijing* 100049, *China*
[4] *Institute of Nuclear and New Energy Technology, Collaborative Innovation Center of Advanced Nuclear Energy Technology, Key Laboratory of Advanced Reactor Engineering and Safety of Ministry of Education, Tsinghua University, Beijing* 100084, *China*
[5] *CAS Center for Excellence in Topological Quantum Computation, University of Chinese Academy of Sciences, Beijing* 100190, *China*

(Received 24 February 2022; revised manuscript received 23 April 2022; accepted manuscript online 7 May 2022)

Recently, a Rydberg atom-based mixer was developed to measure the phase of a radio frequency (RF) field. The phase of the signal RF (SIG RF) field is down-converted directly to the phase of a beat signal created by the presence of a local RF (LO RF) field. In this study, we propose that the Rydberg atom-based mixer can be converted to an all-optical phase detector by amplitude modulation (AM) of the LO RF field; that is, the phase of the SIG RF field is related to both the amplitude and phase of the beat signal. When the AM frequency of the LO RF field is the same as the frequency of the beat signal, the beat signal will further interfere with the AM of the LO RF field inside the atom, and then the amplitude of the beat signal is related to the phase of the SIG RF field. The amplitude of the beat signal and the phase of the SIG RF field show a linear relationship within the range of 0 to $\pi/2$ when the phase of the AM is set with a difference $\pi/4$ from the phase of the LO RF field. The minimum phase resolution can be as small as 0.6° by optimizing the experimental conditions according to a simple theoretical model. This study will expand and contribute to the development of RF measurement devices based on Rydberg atoms.

Keywords: quantum sensor, phase detector, Rydberg atoms, micorwave, electromagnetically induced transparency, amplitude modulation

PACS: 07.07.Df, 84.40.–x, 42.50.–p **DOI:** 10.1088/1674-1056/ac6dbb

1. Introduction

The Rydberg atom-based radio-frequency (RF) sensor utilizes electromagnetically induced transparency (EIT) and Autler–Townes (AT) splitting to enable an optical readout of the RF electric field.[1–4] This approach offers a direct international system of units (SI) traceable, a broad frequency range, and a self-calibrated measurement of the RF electric field.[1–6] The Rydberg atom-based RF sensor has made rapid progress in the past decade and provided new detection capabilities beyond the traditional antenna and other RF detectors.[7–15] The Rydberg atom-based RF sensor has also been used as atomic receivers to demonstrate RF communication.[16–19]

The technique for precisely measuring the phases of RF fields is important and applied broadly in antenna metrology, radar, remote sensing, and various other fields. Simons *et al.* successfully converted the Rydberg atom-based sensor to a mixer and directly measured the phase of the signal RF (SIG RF) electric field.[20] The phase of the SIG RF field is down-converted directly to the phase of the intermediate frequency (IF) beat signal (on the order of kHz), which is created by the presence of a local RF (LO RF) field.[20–22] In the present Rydberg atom-based mixer schemes, the amplitude of the beat signal remains constant, and the phase of the SIG RF field can be read out by comparison with another same frequency reference waveform,[20–22] for example, combines an RF combiner or a spectrum analyzer with the mixer.

In this study, we propose the conversion of the Rydberg atom-based mixer to an all-optical Rydberg atom-based phase detector. Through the amplitude modulation (AM) of the LO RF field with the frequency of the beat signal in the Rydberg atom-based mixer, the amplitude of the beat signal was changed and related to the phase of the SIG RF field. We present a more convenient readout for RF phase measurements after studying the relationship between the output voltage of the phase detector and the phase of the SIG RF field. Furthermore, we use the Rydberg atom-based phase detector to realize a sub-degree phase resolution.

†Corresponding author. E-mail: fxie@tsinghua.edu.cn
‡Corresponding author. E-mail: zpzhong@ucas.ac.cn

© 2022 Chinese Physical Society and IOP Publishing Ltd

2. Theory

Figure 1(a) shows the atomic energy levels applied in this study. The energy levels are ^{87}Rb, $5S_{1/2}(F=2)$, $5P_{3/2}(F'=3)$, $53D_{5/2}(F=4)$ and $54P_{3/2}(F=3)$ corresponding to $|1\rangle$, $|2\rangle$, $|3\rangle$, $|4\rangle$, respectively. Rydberg EIT occurs when the frequency of the weak probe field is scanned near the resonant transition of $|1\rangle$ to $|2\rangle$ in the presence of a strong coupling field coupled with $|2\rangle$ to $|3\rangle$ transition. The LO RF field resonates with the Rydberg transition $|3\rangle$ and $|4\rangle$. The frequency difference between the LO RF field and SIG RF field is $\Delta\omega$. The electric field experienced by the atoms is defined as $E_{\rm atom}$ and the low frequency term $E_{\rm mod}$ is given by[20]

$$E_{\rm mod}=\sqrt{E_{\rm LO}^2+E_{\rm SIG}^2+2E_{\rm LO}E_{\rm SIG}\cos(\Delta\omega t+\Delta\phi)}, \quad (1)$$

where $E_{\rm LO}$ and $E_{\rm SIG}$ are the electric field amplitudes of the LO RF and SIG RF field, respectively. $\Delta\phi=\phi_{\rm SIG}-\phi_{\rm LO}$ is the difference between the SIG RF field phase $\phi_{\rm SIG}$ and the LO RF field phase $\phi_{\rm LO}$, and $\phi_{\rm LO}$ is set to zero for simplicity.

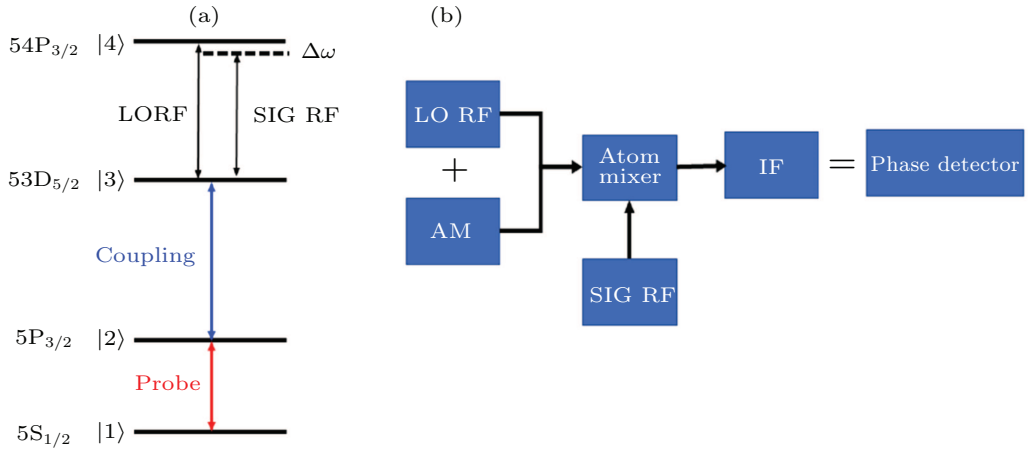


Fig. 1. Basic principle of the Rydberg atom-based phase detector. (a) Levels scheme. (b) Block diagram of the Rydberg atom-based "phase detector", which combines the Rydberg atom-based "mixer" with AM of the LO RF field; the phase of the SIG RF is carried in the oscillation amplitude of the transmittance of the probe laser (known as the beat signal).

The RF field causes AT splitting of the EIT signal, and the transmittance of the probe light $T_{\rm p}$ is proportional to the amplitude of the RF field within a certain range.[23] For a weak SIG RF field, where $E_{\rm SIG}\ll E_{\rm LO}$, Eq. (1) can be written as[20]

$$T_{\rm p}\propto E_{\rm mod}\propto E_{\rm LO}+E_{\rm SIG}\cos\left(\Delta\omega t+\phi_{\rm SIG}\right), \quad (2)$$

where $T_{\rm p}$ shows periodic oscillation (known as the beat signal) with constant amplitude. Because the beat signal is an IF signal (on the order of kHz), $\phi_{\rm SIG}$ can be read out by comparison with another same frequency reference waveform after the beat signal passes through the photodector, for example, assemble with an RF combiner.

Figure 1(b) shows the transformation process of the Rydberg atom-based mixer to a phase detector. The amplitude of the LO RF field was periodically modulated with the frequency of the beat signal. The modulation depth and modulation phase are defined as $D_{\rm AM}$ and $\phi_{\rm AM}$, respectively. Then, $T_{\rm p}$ can be written as

$$\begin{aligned}T_{\rm p}\ &\propto\ E_{\rm mod}\propto D_{\rm AM}\times E_{\rm LO}\cos\left(\Delta\omega t+\phi_{\rm AM}\right)\\&\quad+E_{\rm SIG}\cos\left(\Delta\omega t+\phi_{\rm SIG}\right).\end{aligned} \quad (3)$$

If $D_{\rm AM}$, $E_{\rm LO}$ and $E_{\rm SIG}$ satisfy the relationship of $D_{\rm AM}\times E_{\rm LO}\approx E_{\rm SIG}$. Then Eq. (3) can be further simplified to

$$T_{\rm p}\ \propto\ E_{\rm mod}\propto 2E_{\rm SIG}\cos\frac{\phi_{\rm AM}-\phi_{\rm SIG}}{2}$$

$$\times\cos\left(\Delta\omega t+\frac{\phi_{\rm AM}+\phi_{\rm SIG}}{2}\right). \quad (4)$$

Finally, since the $\cos(\Delta\omega t+\frac{\phi_{\rm AM}+\phi_{\rm SIG}}{2})$ term only changes the phase of the beat signal and the $2E_{\rm SIG}\cos\frac{\phi_{\rm AM}-\phi_{\rm SIG}}{2}$ term really affects the amplitude of the beat signal, the change of the beat signal amplitude only depends on $\cos\frac{\phi_{\rm AM}-\phi_{\rm SIG}}{2}$. The amplitude of the beat signal $A_{\rm Beat}$ satisfies a very simple relationship with $\phi_{\rm SIG}$,

$$A_{\rm Beat}\propto\cos\frac{\phi_{\rm AM}-\phi_{\rm SIG}}{2}. \quad (5)$$

It can be seen that we can directly extract $\phi_{\rm SIG}$ through $A_{\rm Beat}$ in the experiment. When $E_{\rm LO}$ is modulated, only the amplitude of the beat signal is affected, and the phase information of the SIG RF field is completely inherited. It can be seen from Eq. (3) that in addition to $\phi_{\rm SIG}$, all of $D_{\rm AM}$, $\phi_{\rm AM}$, $E_{\rm LO}$ and $E_{\rm SIG}$ will affect the amplitude of the beat signal. Therefore, these quantities should remain stable and this is relatively easy to realize in practical applications. For example, $E_{\rm SIG}$ can be attenuated to a fixed value and then sent to the atomic sensor. Consequently, the relationship between $\phi_{\rm SIG}$ and output voltage of the phase detector can be obtained. Thus, our method is to directly compare the reference phase with $\phi_{\rm SIG}$ inside the atomic mixer. It avoids the perturbation that may be encountered in the transmission process of the beat signal to the RF combiner in the traditional phase detector scheme.

3. Experimental setup

Figure 2 schematically shows the experimental setup, which is based on the Rydberg atomic sensor and mixer. A weak probe light with $\lambda_p = 780$ nm was generated using an external cavity semiconductor laser (DL100, Toptica), and the frequency was locked on the resonance transition of $|1\rangle$ to $|2\rangle$ using the Zeeman modulation saturated absorption spectrum (SAS).[24] A relatively stronger coupling light with $\lambda_c = 480$ nm was generated using a frequency-doubled diode laser (TA-SHG-Pro, Toptica), and the frequency was locked on the resonance transition of $|2\rangle$ to $|3\rangle$ using the Zeeman modulation Rydberg EIT spectrum.[25] The linewidths of all the lasers were estimated to be less than 500 kHz using the linewidth of the Rydberg EIT with 494 kHz in cold atom samples.[25] The minimum Allen variance $\sigma(\tau)_{\text{laser}}$ of lasers was approximately 7.3×10^{-11} at 8 s for laser stabilization.[26] The probe light was focused to an 800 μm $1/e^2$ diameter using an achromatic lens with power $I_p = 25$ μW. The coupling light with power $I_c = 30$ mW was focused to a 900 μm $1/e^2$ diameter. The probe light and coupling light were both linearly polarized and were counter-propagating in the Rb cell. Then, the intensity of the probe beam passing through the cell was detected using a photodiode (PD) and sent to the lock-in amplifier (LI5640, NF Corporation), and finally recorded by the oscilloscope.

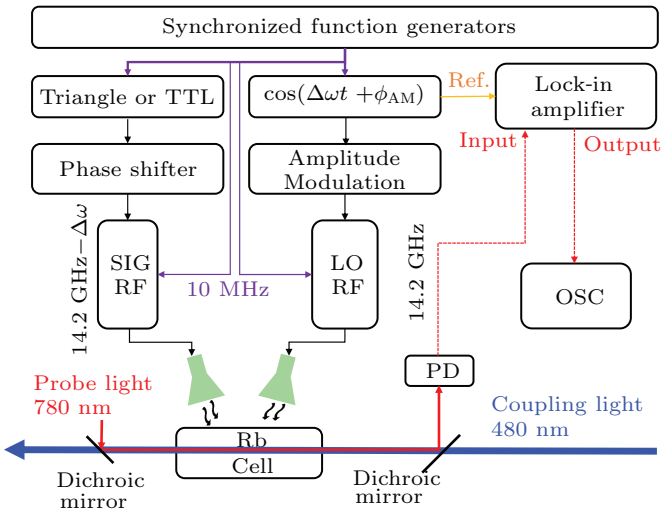


Fig. 2. Schematic of the experimental setup for the Rydberg atom-based phase detector. PD denotes the photodetector, purple lines denote the rubidium clock synchronization signals, orange line denotes the reference signal of the lock-in amplifier, and the red dotted line denotes the signal received by the PD and the output of the lock-in amplifier. OSC denotes the oscilloscope.

Here, we used two signal generators to produce the two microwave fields. The first signal generator (8340 B, Keysight Technologies) was used to generate the LO RF field at 14.233 GHz to drive the Rydberg transition $|3\rangle$ to $|4\rangle$. The second signal generator (E8257 D, Keysight Technologies) was used to apply the SIG RF field at 14.233 GHz $-\Delta\omega$ (where $\Delta\omega$ can vary from 1 kHz to 100 kHz). The outputs of the two signal generators were connected to two separate horn antennas (LB-62-10-C-SF) that radiate the microwaves toward the cylinder Rb cell (diameter 25 mm and length 75 mm), and the antennas were placed far away from the Rb cell to satisfy the far-field condition. The two signal generators were triggered by the same GPS (Global Positioning System)-tamed 10 MHz Rb clock (FS725, Stanford) to keep the frequency drift of both signal generators to a very low level. The tested minimum Allen variance $\sigma(\tau)_{\text{clock}}$ of the 10 MHz Rb clock was 1.44×10^{-14} after being tamed for 24 h by the GPS. The frequency drifts of the two microwaves were 10^{-2} Hz within 2 h (compared with 1 Hz frequency drifts after being triggered by the Rb clock inside the signal generator within 2 h), which was sufficiently stable for our experiments.[23] The polarizations of the two microwave electric fields were the same as those of the probe and coupling beams and propagated in a vertical direction to the two laser beams.

Next, we describe the conversion of the Rydberg atom-based mixer to a phase detector. A function generator generated a sinusoidal signal with the same frequency as the beat signal to modulate the amplitude of the LO RF field. The amplitude and phase of the modulation signal can both be controlled. In addition, the output signal of the function generator was also sent to the lock-in amplifier as a reference signal to demodulate the amplitude of the beat signal and then recorded by the oscilloscope. Another function generator applied a triangular wave signal or a transistor-transistor logic (TTL) signal to trigger a phase shifter to change the phase of the SIG RF field ϕ_{SIG}. Specifically, when the voltage of the triangular wave or the TTL signal changes from -0.5 V to 0.5 V, ϕ_{SIG} can change linearly within the set range.

4. Results and discussion

First, we discuss the effect of E_{LO} and E_{SIG} on T_p. Then, we describe the influence of the amplitude modulation of the LO RF field on the performance of the phase detector, including the phase ϕ_{AM} and depth D_{AM} of the amplitude modulation of the LO RF field. Furthermore, we study phase resolution capability of the phase detector.

We briefly discuss the relationship between the transmittance of the probe light T_p and the RF electric field amplitude experienced by the atoms E_{LO} (or E_{SIG}) when the probe light and the coupling light are locked at the EIT resonance frequency. The results show that T_p and E_{LO} (or E_{SIG}) satisfy a monotonic proportional relationship when 0.8 mV/cm $\leq E_{\text{LO}}$ (or E_{SIG}) $\leq$ 20 mV/cm. When E_{LO} (or E_{SIG}) is less

than 0.8 mV/cm or greater than 20 mV/cm, T_p will not change significantly with E_{LO} (or E_{SIG}). Therefore, in the following experiments, we will study and optimize the performance of phase detector by choosing E_{LO} and E_{SIG} in the range of 0.8–20 mV/cm.

To study the relationship between ϕ_{AM} and ϕ_{SIG} under LO RF field amplitude modulation, we used a phase shifter to change ϕ_{SIG} continuously over 4π and set $\phi_{LO} = 0$ for simplicity. The data were obtained with a beat frequency $\Delta\omega = 1$ kHz. The black, blue, and red solid lines in Fig. 3 represent the experimental results with $\phi_{AM} = 0, \pi/4$, and π, respectively. The dotted lines represent the corresponding theoretical calculation results in Eq. (5). Therefore, for the convenience of comparison, a coefficient calibration was performed on the theoretical calculation results. As shown in Fig. 3, it is found that the amplitude of the beat signal A_{Beat} and ϕ_{SIG} show a monotonic relationship. Furthermore, the output amplitude of the beat signal and ϕ_{SIG} show a approximate linearity from 0 to $\pi/2$ when $\phi_{AM} = \pi/4$, while the traditional commercial phase detector can realize the linear region of 2π. Therefore, ϕ_{SIG} can be directly converted into a voltage signal, and then the Rydberg atom-based mixer can act as a phase detector. From Fig. 3, we can also find that if we change ϕ_{AM}, the amplitude of the beat signal will be only related to the difference between ϕ_{SIG} and ϕ_{AM}. For example, when the amplitude of the beat signal is the positive largest, the difference between ϕ_{SIG} and ϕ_{AM} is always $k\pi, k = 0, \pm2, \pm4, \ldots$, as shown in Fig. 3. This is also consistent with Eq. (5). Therefore, from this method, we can clearly know that even if ϕ_{AM} changes, ϕ_{SIG} can also be deduced from the amplitude of the beat signal A_{Beat}. The calculation result of Eq. (5) is in agreement with the experimental results. The slight difference may owe to the over-simplification of Eq. (5), for example, T_p is not strictly linear with E_{LO} or E_{SIG}. However, this does not affect the use of the phase detector because the output of the phase detector can be calibrated before the application. The results in Fig. 3 can be repeated when $\Delta\omega$ varies from 1 kHz to 100 kHz, where the upper limit of 100 kHz is limited by the bandwidth of the lock-in amplifier. At 100 kHz, the signal is still clear, which shows that the applicable frequency range of this method is very large.

Next, we study the influence of the amplitude modulation depth of the local RF field D_{AM} on the output signal of the phase detector, and the results are given in Fig. 4. The results show that when $\Delta\phi_{SIG}$ is fixed at 10° and $\Delta\omega = 100$ kHz, the change in the phase detector output is proportional to the modulation depth D_{AM} within 10%–90%. When D_{AM} is less than 10%, the signal cannot be demodulated, and the error of the system at each D_{AM} is very small. The results show that the output of the phase detector is proportional to D_{AM}, and it has a wide range of D_{AM} and high repeatability and stability. The red dotted line was calculated using Eq. (3) with the same parameters as in the experiment and was qualitatively consistent with the experimental results. Noted that the theoretical calculation was normalized to facilitate comparison with the experimental results. Although the phase detector can work in a wide range of D_{AM}, in order for both to satisfy $E_{LO} \gg E_{SIG}$ and $E_{LO} \times D_{AM} \approx E_{SIG}$ at the same time, we choose $D_{AM} = 20\%$ in the following experiments.

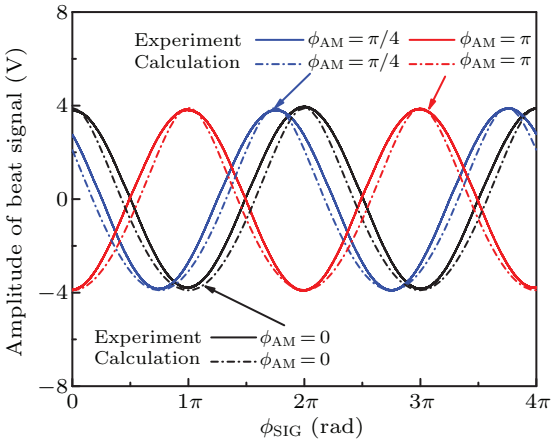


Fig. 3. Examples of the Rydberg atom-based phase detector; experimental parameters: $E_{LO} = 10.14$ mV/cm, $E_{SIG} = 2.75$ mV/cm, $\Delta\omega = 1$ kHz, and the modulation depth D_{AM} is 20%; assuming that $\phi_{LO} = 0$. The black, blue, and red solid lines represent the experimental results with $\phi_{AM} = 0, \pi/4$, and π, respectively; each curve corresponds to 32 averages to improve the signal-to-noise ratio. The dotted lines represent the corresponding theoretical calculation results in Eq. (5). Theoretical calculation amplitude is normalized to facilitate the comparison with the experimental results.

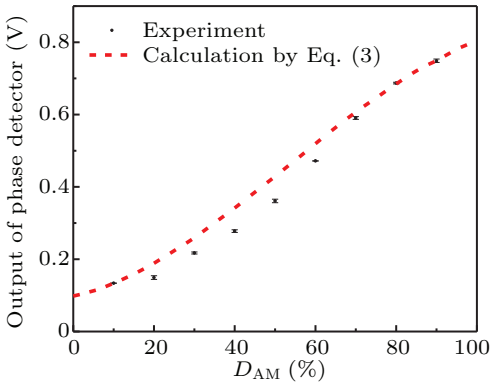


Fig. 4. Relationship between the beat frequency oscillation amplitude and the modulation depth D_{AM}, where $\Delta\phi_{SIG} = 10°$. Black solid circles denote the experimental results with parameters $E_{LO} = 10.14$ mV/cm, $E_{SIG} = 2.75$ mV/cm, and $\Delta\omega = 100$ kHz; red dotted line is calculated using Eq. (3). The theoretical calculation is normalized to facilitate the comparison with the experimental results, and the calculation parameters are the same as the experimental parameters.

Finally, we demonstrate the phase resolution capability of the Rydberg atom-based phase detector by changing the phase difference of the SIG RF field $\Delta\phi_{SIG}$ and measuring the output voltage of the phase detector. Based on Eq. (3), A_{Beat} is most sensitive to ϕ_{SIG} when $D_{AM} \times E_{LO} \approx E_{SIG}$, therefore we choose the experimental parameters: $E_{LO} = 10.14$ mV/cm, $E_{SIG} = 2.75$ mV/cm, and the modulation depth $D_{AM} = 20\%$. In the meantime, ϕ_{AM} was set to $\pi/4$ to obtain the maximum slope of A_{Beat} to ϕ_{SIG} near $\phi_{SIG} = 0$ as shown in Fig. 3. The

data obtained with the beat frequency $\Delta\omega = 1$ kHz and averaged over 128 sets of data to enhance the signal-to-noise ratio (SNR) of the readout. Figure 5(a) shows the output voltage of the corresponding phase detector when $\Delta\phi_{\rm SIG}$ is taken as 12°, 10°, 8°, 5°, 2°, and 1°, respectively. It can be seen that the phase detector still has a good readout when $\Delta\phi_{\rm SIG}$ is set to 1°. Figure 5(b) shows the corresponding analysis results in Fig. 5(a). The horizontal axis represents $\Delta\phi_{\rm SIG}$, and the vertical axis corresponds to the amplitude of output signal of the phase detector. The black hollow circles are the experimental results corresponding to Fig. 5(a), and the red solid line is the result of a linear fitting that crosses the 0 points. After analyzing the average value and error of the corresponding phase detector output voltage at high level and low level in the experiment, the achievable phase resolution is 0.6°, while Ref. [13] obtained a resolution of 0.8° using the superheterodyne method, and a traditional commercial phase detector can achieve the phase resolution of about 1°.[27]

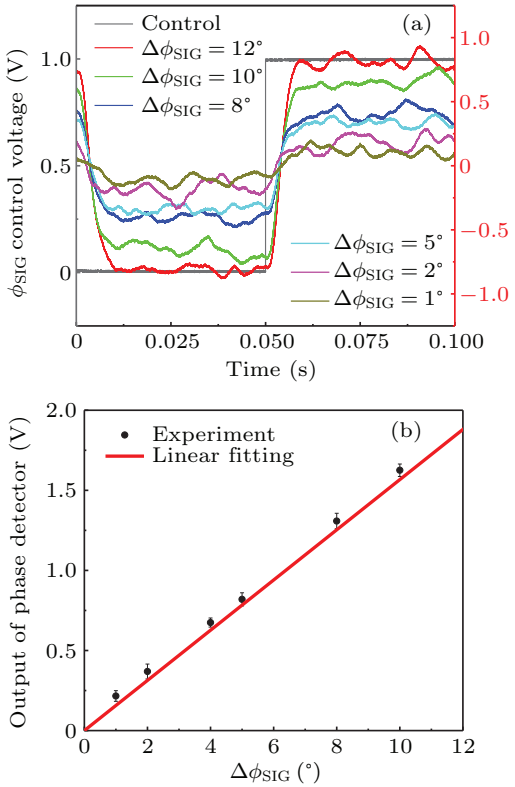


Fig. 5. Relationship between the beat frequency oscillation amplitude and the set phase difference. (a) Phase control and reaction of the Rydberg atom-based phase detector. Black solid line is the control voltage of the phase shifter; −0.5–0.5 V corresponds to the set phase difference. Red line, green line, blue line, cyan line, magenta line and dark yellow line represent the output voltage of the corresponding phase detector when $\Delta\phi_{\rm SIG}$ is 12°, 10°, 8°, 5°, 2° and 1°, respectively. Each curve corresponds to 128 averages to enhance SNR. By setting $\Delta\phi_{\rm SIG}$, $\phi_{\rm SIG}$ can jump back and forth with the value of $\Delta\phi_{\rm SIG}$. Specifically, 0.5 V phase control corresponds to $\phi_{\rm SIG} = \Delta\phi_{\rm SIG}/2$, and −0.5 V phase control corresponds to $\phi_{\rm SIG} = -\Delta\phi_{\rm SIG}/2$; phase difference between the amplitude modulation of the local field and the phase of the local field is fixed to $\pi/4$; experimental parameters: $E_{\rm LO} = 10.14$ mV/cm, $E_{\rm SIG} = 2.75$ mV/cm, $\Delta\omega = 1$ kHz, and the modulation depth $D_{\rm AM} = 20\%$. (b) Relationship between the beat frequency oscillation amplitude and the set phase difference. Black hollow circle denotes the experimental result corresponding to (a); red solid line denotes a linear fitting that crosses the 0 points. The experimental data are not collected in the same day, so the data of Figs. 3 and 5 cannot be directly compared.

5. Conclusion

We have converted the Rydberg atom-based mixer to an all-optical Rydberg atom-based phase detector by the amplitude modulation of the LO RF field; that is, the phase of the SIG RF field can be directly converted into a voltage signal. The amplitude of the beat signal $A_{\rm Beat}$ and the phase of the SIG RF field $\phi_{\rm SIG}$ show a monotonic relaionship when the amplitude of the local RF field is modulated by the frequency of the beat signal. The output voltage of the phase detector and $\phi_{\rm SIG}$ show a linear relationship within the range of 0–$\pi/2$ of the SIG RF field phase when $\phi_{\rm AM}$ is set with a difference of $\pi/4$ from the phase of the local RF field. A sub-degree phase resolution is also achieved by optimizing the experimental conditions according to a simple theoretical model. Because the Rydberg atom-based phase detector is an optical readout, it is better than the traditional phase detector in noise suppression. This work will expand and contribute to the development of RF measurement devices based on Rydberg atoms.

Acknowledgements

Project supported by the National Key Research and Development Program of China (Grant Nos. 2017YFA0304900 and 2017YFA0402300), the Beijing Natural Science Foundation (Grant No. 1212014), the National Natural Science Foundation of China (Grant Nos. 11604334, 11604177, and U2031125), the Key Research Program of the Chinese Academy of Sciences (Grant No. XDPB08-3), the Open Research Fund Program of the State Key Laboratory of Low-Dimensional Quantum Physics (Grant No. KF201807), the Fundamental Research Funds for the Central Universities, and Youth Innovation Promotion Association CAS.

References

[1] Sedlacek J A, Schwettmann A, Kübler H, Löw R, Pfau T and Shaffer J P 2012 *Nat. Phys.* **8** 819
[2] Fancher C T, Scherer D R, John M C S and Marlow B L S 2021 *IEEE Trans. Quantum Eng.* **2** 3501313
[3] Fan H Q, Kumar S, Sedlacek J A, Kübler H, Karimkashi S and Shaffer J P 2015 *J. Phys. B: At. Mol. Opt. Phys.* **48** 202001
[4] Holloway C L, Gordon J A, Simons M T, Fan H Q, Kumar S, Shaffer J P, Anderson D A, Schwarzkopf A, Miller S A and Thaicharoen N 2015 *IEEE International Symposium on Electromagnetic Compatibility (EMC)*, August 16–22, 2015, Germany, pp. 467–472
[5] Anderson D A, Sapiro R E and Raithel G 2021 *IEEE Trans. Antennas Propag.* **69** 2455
[6] Holloway C L, Gordon J A, Jefferts S, Schwarzkopf A, Anderson D A, Miller S A, Thaicharoen N and Raithel G 2014 *IEEE Trans. Antennas Propag.* **62** 6169
[7] Simons M T, Gordon J A, Holloway C L, Anderson D A, Miller S A and Raithel G 2016 *Appl. Phys. Lett.* **108** 174101
[8] Zhang L J, Jia Y, Jing M Y, Guo L P, Zhang H, Xiao L T and Jia S T 2019 *Laser Phys.* **29** 035701
[9] Fan H Q, Kumar S, Kübler H and Shaffer J P 2016 *J. Phys. B: At. Mol. Opt. Phys.* **49** 104004
[10] Kumar S, Fan H Q, Kübler H, Jahangiri A J and Shaffer J P 2017 *Opt. Express* **25** 8625
[11] Kumar S, Fan H Q, Kübler H, Sheng J T and Shaffer J P 2017 *Sci. Rep.* **7** 1

[12] Liao K Y, Tu H T, Yang S Z, Chen C J, Liu X H, Liang J, Zhang X D, Yan H and Zhu S L 2020 *Phys. Rev. A* **101** 053432
[13] Jing M Y, Hu Y, Ma J, Zhang H, Zhang L J, Xiao L T and Jia S T 2020 *Nat. Phys.* **16** 911
[14] Jia F D, Liu X B, Mei J, Yu Y H, Zhang H Y, Lin Z Q, Dong H Y, Zhang J, Xie F and Zhong Z P 2021 *Phys. Rev. A* **103** 063113
[15] Liu X B, Jia F D, Zhang H Y, Mei J, Yu Y H, Liang W C, Zhang J, Xie F and Zhong Z P 2021 *AIP Adv.* **11** 085127
[16] Meyer D H, Cox K C, Fatemi F K and Kunz P D 2018 *Appl. Phys. Lett.* **112** 211108
[17] Deb A and Kjaergaard N 2018 *Appl. Phys. Lett.* **112** 211106
[18] Holloway C L, Simons M T, Gordon J A and Novotny D 2019 *IEEE Antennas Wirel. Propag. Lett.* **18** 1853
[19] Song Z F, Liu H P, Liu X C, Zhang W F, Zou H Y, Zhang J and Qu J F 2019 *Opt. Express* **27** 8848
[20] Simons M T, Haddab A H, Gordon J A and Holloway C L 2019 *Appl. Phys. Lett.* **114** 114101
[21] Gordon J A, Simons M T, Haddab A H and Holloway C L 2019 *AIP Adv.* **9** 045030
[22] Robinson A K, Prajapati N, Senic D, Simons M T and Holloway C L 2021 *Appl. Phys. Lett.* **118** 114001
[23] Jia F D, Zhang H Y, Liu X B, Mei J, Yu Y H, Lin Z Q, Dong H Y, Liu Y, Zhang J, Xie F and Zhong Z P, *et al.* 2021 *J. Phys. B: At. Mol. Opt. Phys.* **54** 165501
[24] Weis A and Derler S 1988 *Appl. Opt.* **27** 2662
[25] Jia F D, Zhang J, Zhang L, Wang F, Mei J, Yu Y H, Xie F and Zhong Z P 2020 *Appl. Opt.* **59** 2108
[26] Jia F D, Yu Y H, Liu X B, Zhang X, Zhang L, Wang F, Mei J, Zhang J, Xie F and Zhong Z P 2020 *Appl. Opt.* **59** 8253
[27] Chen H and Chan E H W 2021 *IEEE Photon. J.* **13** 7900709